Avelhaneda Mallmann et al. *New Zealand Journal of Forestry Science* (2025) 55:9
https://doi.org/10.33494/nzjfs552025x411x
E-ISSN: 1179-5395
published on-line: 14/05/2025

RESEARCH ARTICLE Open Access

New Zealand Journal of Forestry Science

Uniformity measures for young *Eucalyptus* sp. plantations using attributes extracted from UAV flights

Adriane Avelhaneda Mallmann[1]*, Ana Paula Dalla Corte[1], Alexandre Behling[1], Rubén Manso[2], Kauana Engel[1], Claiton Nardini[1]*, Iací Dandara Santos Brasil[1], José Augusto Spiazzi Favarin[1], Jonathan William Trautenmüller[1] and Gabriel Agostini Orso[1]

[1] Department of Forest Sciences, Federal University of Paraná, Av. Pref. Lothário Meissner, 900, Jardim Botânico, Campus III, 80210-170 Curitiba, PR, Brazil
[2] Forest Research, Bush Estate, Roslin, Midlothian, EH25 9SY, Scotland, UK

*Corresponding author: mallmann.adriane@gmail.com / claitonardini@gmail.com

(Received for publication 2 August 2024; accepted in revised form 14 April 2025)
Editor: Euan G. Mason

Abstract

Background: Studies show that forest uniformity has a direct correlation with productivity, and uniformity measures can serve as indicators of the silvicultural quality of plantations. In this context, this work aimed to determine uniformity and survival in young *Eucalyptus* sp. plantations using attributes obtained from passive sensors boarded on Unmanned Aerial Vehicles (UAV).

Methods: Tree height was underestimated by the UAV compared to those measured in the Quality Forest Inventory (QFI). Thus, a correction factor applied to size classes was proposed to estimate these heights. The plantations' uniformity was obtained through the uniformity indices (UI). The UIs were spatialised and integrated, resulting in two uniform surfaces, with and without planting failures.

Results: The UAV survival estimates did not show significant differences compared to the inventory estimates at the 1% or the 5% significance levels. The classification of uniformity surfaces showed that the *Eucalyptus saligna* Sm plantation was the least uniform compared to the *E. grandis* W. Hill × *E. urophylla* S. T. Blake plantations.

Conclusions: Measures of survival and uniformity by the UAV can be jointly employed to generate uniformity surfaces and to determine the areas that need more attention from silvicultural management.

Keywords: Forest uniformity, Unmanned Aerial Vehicles, Silvicultural management, Spatial analysis

Introduction

In Brazil, the first commercial plantations of forest species were established as an alternative for the wood supply that came from natural forests, especially the Atlantic Forest (AGEFLOR 2023). Currently, according to IBÁ (2022), in Brazil, forest plantations total about 9.93 million hectares and absorb some 1.88 billion tons of carbon dioxide (CO_2) from the atmosphere.

The area of commercial plantations of the genus *Eucalyptus* sp. has been increasing every year, especially due to the establishment of new plantations (Sanquetta et al. 2018; IBÁ 2019). This highlights the interest in species of this genus in the Brazilian forestry sector, which is internationally recognised for its short rotations and the productivity of its plantations.

The productivity of *Eucalyptus* spp. plantations has increased in recent decades, reaching 38.9 m^3 ha^{-1} $year^{-1}$ in 2021, and maintaining this growth is a challenge for the forestry sector (Gonçalves et al. 2014; IBÁ 2022). Among the factors related to productivity is the structural uniformity of plantations, a factor that has been positively correlated with higher forest productivity (Binkley et al. 2010; Stape et al. 2010; Ryan et al. 2010; Aspinwall et al. 2011, Hakamada et al. 2015a).

The structural uniformity of the stand reflects the environmental conditions in which the plantation grows, the quality of the genetic material employed, the quality of the silvicultural activities applied, and the interactions among these factors (Hakamada et al. 2015a; Soares et al. 2016; Sun et al. 2018). It is important that the determination of structural uniformity be performed early in the first months of planting, as uniformity decreases with the advancing age of the forest stand (Hakamada et al. 2015b; Soares et al. 2016; Sun et al. 2018).

Information about the uniformity of plantations provides greater detail about productive areas, serving as an indicator of the adequacy of resource supply for growth (Hakamada et al. 2015b, Binkley et al. 2010; Stape et al. 2010) and allowing forest managers to have a broader view of the stand structure. This detailed understanding enables the identification of areas that require greater attention from silvicultural managers and interventions needed in the early years of the plantation (Binkley et al. 2002; Binkley et al. 2010; McGown et al. 2016; Resende et al. 2016; Yáñez et al. 2017; Sun et al. 2018), ensuring the greatest structural uniformity so that the stand can achieve its potential productivity (Luu et al. 2013).

Uniformity can be estimated through uniformity indices (Hakamada et al. 2015a; McGown et al. 2016; Yáñez et al. 2017; Hentz et al. 2018). The calculation of these indices is usually done through sampling data of variables obtained by a conventional forest inventory. However, for large areas with difficult access, the collection of these data can become a costly activity or even unfeasible from a practical and economic point of view.

Remote sensing techniques have been increasingly employed in the forest sector for generation of qualitative and quantitative data. The use of unmanned aerial vehicles (UAV) has been shown to have potential as a tool to conduct forest inventories due to the low cost of operation of this platform in environmental monitoring, the potential to reduce the time to obtain information from the plantations, the possibility of high accuracy of the results, the high spatial and temporal resolution, as well as the high flexibility in the acquisition of images (Corte et al. 2020; Zhang and Kovacs 2012; Salamí et al. 2014; Torresan et al. 2017).

This research differs from other studies due to its specific focus on employing data collected by passive sensors mounted on UAV to calculate survival and uniformity indices in young *Eucalyptus* sp. plantations, whereas most previous research utilised conventional forest inventory methods. Although the existing literature recognises the potential of UAV for forest inventories, there is a notable scarcity of studies in Brazil that integrate UAV technology with uniformity indices, as highlighted by Hentz et al. (2018). By spatially integrating the survival and uniformity indices obtained from UAV data, this research aims to enhance the understanding of plantation dynamics in a way that traditional methods may not capture.

The following study hypothesis was established: "The data collected by passive sensors onboard a UAV can be employed to calculate survival and uniformity indices in young plantations of *Eucalyptus* species as a form of integration or replacement of conventionally applied techniques". This work aims to: a) evaluate the accuracy of using data collected by passive sensors mounted on UAV to express survival and uniformity; comparing the data collected by UAV and data collected by a conventional forest inventory; e b) spatially integrate the survival and uniformity indices calculated from data collected by UAV to obtain uniformity surfaces.

Methods

Area of study

The study sites were in three young plantations of *Eucalyptus* sp. which were selected and made available by Klabin S.A. Klabin S.A. is a forestry company and one of the largest producers and exporters of paper and pulp in Brazil. The study was conducted in the municipalities of Ortigueira and Telêmaco Borba, both located in the state of Paraná, southern region of Brazil. According to the Köppen-Geiger classification, the climate is Cfa, with average annual temperature 18.4 °C and average annual rainfall around 1,378 mm (Climate-Data.Org 2024). Plot B corresponds to a monoclonal plantation of the species *Eucalyptus saligna* Sm., and plots A and C are monoclonal plantations of *E. grandis* W. Hill × *E. urophylla* S. T. Blake. Figure 1 shows the location of the three forest plantations used in this study, with coordinates in UTM - SIRGAS 2000, zone 22 S.

The productive area of plantation A was 14.75 hectares, with soils of the Oxisol and Ultisol classes. In plantation B, the productive area was 38.39 ha, with a predominance of Inceptisol soils. Plantation C presented a productive area of 54.19 ha on Oxisol soils. When the study was carried out, all plantations were approximately one year old and with overlapping canopies in the row and partial overlapping between rows.

Data collection – Quality Forest Inventory (QFI)

The field data were collected in the Quality Forest Inventory (QFI), which is usually carried out by Klabin S.A. when the plantations reach one year of age. The plots were randomly allocated to the plantation and were rectangular in shape, composed of 4 rows with 5 trees each, totalling an average of 20 trees per plot. The spacing between trees was 1.8 m x 3.3 m for plantations B and C, and 1.75 m x 3.42 m for plantation A. Because the configuration of the plots was determined by 4 rows x 5 plants, the plots for plantation A had an area of 120 m^2 and the plots for plantations B and C had an area of 119 m^2.

In the field data collection (QFI), all trees in each plot were measured. In plantation A, 61 trees were sampled in 3 plots, in plantation B, 261 trees in 13 plots, and in plantation C, 222 trees in 11 plots.

In the QFI, the trees in the plots were measured for their diameter at breast height (DBH), 1.30 meters from the ground, and total height (H). The DBH was measured with a metric measuring tape, and H was measured with a Haglöf Vertex IV® hypsometer, at a distance of 20 m

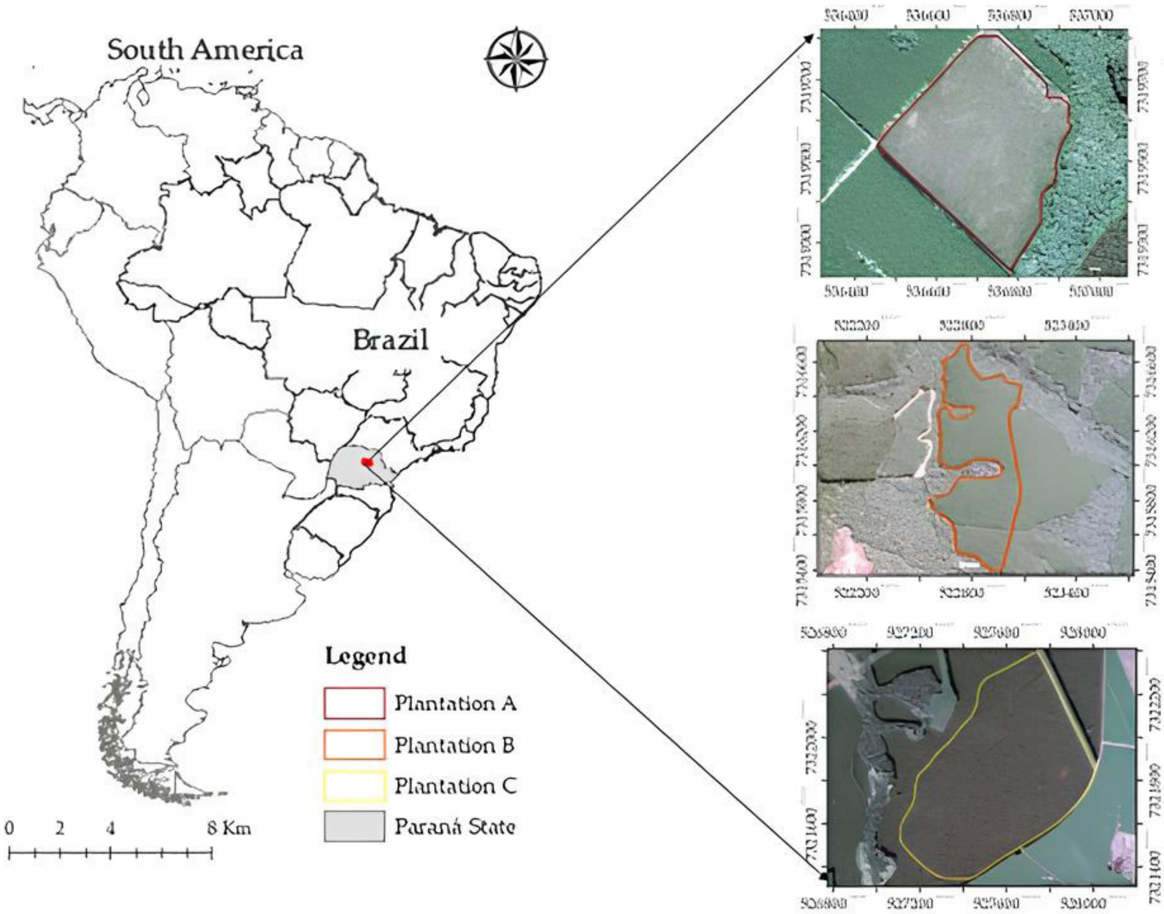

FIGURE 1: *Eucalyptus* plantations located in State of Paraná, Brazil.

from the tree. In addition, the geographic position of the plot was collected with a Garmin 62CSX GPS. According to the owner's manual of the GPSMAP 62 series, the margin of error for exact location is ± 12 ft (or 3.66 m).

Data collection

The flights were performed with the platforms and sensors provided by Klabin S.A. (Table 1). In plantation A and C, the Parrot Disco platform was employed, with the Sequoia multispectral sensor, and in plantation B the Phantom platform with the RGB sensor was employed. The use of different platforms did not interfere in obtaining the cartographic products, since only the RGB bands were employed in image processing for both sensors.

The acquisition of the UAV aerial images was performed on days with clear skies within a flight window between 9 am and 3 pm. The flight path employed was simple acquisition, and the flight height employed was 120 meters, respecting the current legislation of the Brazilian National Civil Aviation Agency.

Data processing

Stage 1: The raw images from the UAV flights were imported and processed in PiX4D software. As a result of the processing, the following cartographic products were obtained: Digital Elevation Model (DEM); Digital Surface Model (DSM); and orthophoto mosaic, also called orthomosaic.

Stage 2: In the GIS environment (ArcMap 10.4.1), with the Raster Calculator tool, the following band math was performed: "DSM - DEM", using the models obtained in Stage 1. The result of the subtraction (DSM - DEM) generated the cartographic product Canopy Height Model or Normalized Digital Surface Model (CHM).

Stage 3: In GIS environment, the delimitation of rectangular plots, as well as their trees, was established through the vectorisation performed by photointerpretation on the orthophotos of each plantation, generated in Stage 1. The allocation of these plots occurred randomly, characterising the simple random sampling system. These plots, vectorised by photointerpretation, were divided into two groups, as follows:

Sampling V1: Plots with the same location and size of the plots coming from QFI, employed in the comparison of the uniformity indices UAV x QFI.

Sampling V2: Plots that did not have the same location as the QFI plots, which were employed to calculate uniformity indices and spatialisation of uniformity surfaces.

TABLE 1: Information on UAV flights over *Eucalyptus* sp. plantations.

Information	Plantation A	Plantation B	Plantation C
Date of flight	May/19	Nov/18	Nov/18
Flight height (m)	120	120	120
Platform	Parrot Disc	Phantom	Parrot Disc
Sensor	Sequoia	RGB	Sequoia
Spatial resolution (cm)	4.5	3.0	4.5
Coverage (%)[1]	70 x 70	70 x 70	70 x 70

[1]Lateral and longitudinal coverage of the images.

The variation in the number of plots in each plantation in the QFI and V1 sampling is linked to the number of QFI plots made available by Klabin S.A., and the variation in the number of plots in the V2 sampling is linked to the size of each plantation (Table 2).

Stage 4: In the plots (UAV) that had their respective plots in the field (QFI), the canopy delineation was performed by photointerpretation, and then their areas were calculated.

Stage 5: In GIS environment, with the Extract Values to Points tool the tree heights of each plot were extracted, using the tree position and the CHM.

Stage 6: The allocation of the planting fault points within the total area of each plantation was conducted by vectorisation of circular plots of 1 hectare that coincided with the central location of the field plots (QFI) and identification of the points of plantation failure. Planting gaps were defined as the absence of trees in the planting line, and their identification was performed by photointerpretation.

Thus, through the Stage 1 to Stage 4 work sequence, the following attributes were extracted: height (H, m); canopy area (Ca, m^2); failure in plots (absence of trees on the plot) (Fp, n ha^{-1}); and failure census (count of failures in the area) (Fc, n ha^{-1}) (Figure 2).

An exploratory analysis of the data revealed that, in comparison to the heights from the QFI, the heights extracted by the UAV presented a systematic error with a tendency to underestimate the measurements. To overcome this limitation, the heights extracted by the UAV were adjusted based on plots sampled in the field. For this, the correction factors were obtained per size class of height (R_j, Equation 1) and the correction of UAV heights was performed using Equation 2.

TABLE 2: Number of plots employed in plantations of *Eucalyptus* sp.

Sampling	Plantation A	Plantation B	Plantation C
QFI and Sampling V1	3	13	11
Sampling V2	20	30	30

FIGURE 2: Working sequence for extracting UAV attributes.

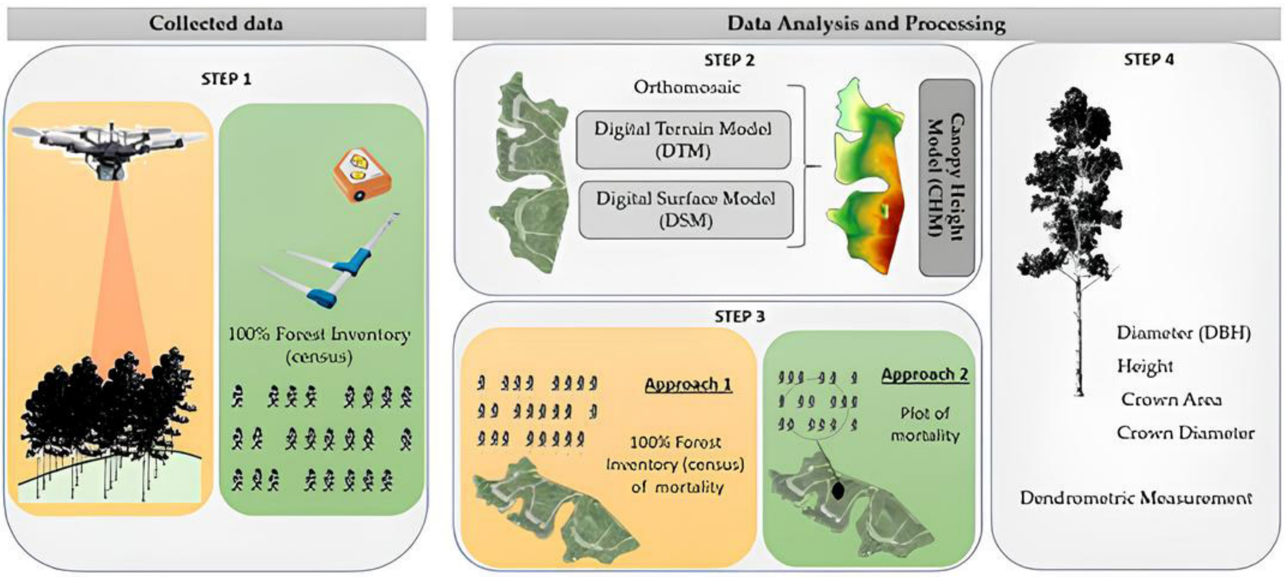

$$R_j = \frac{\sum_{i=1}^{n_j} h_{oi}}{\sum_{i=1}^{n_j} h_{ei}} \quad (1)$$

$$h_{ei_{Corr}} = h_{ei}\, R_j \quad (2)$$

Where: R_j is class *j* ratio; h_{oi} is the height obtained from QFI in class *j*, and h_{ei} is the height extracted by the UAV in class *j*. The term $h_{ei_{Corr}}$ is the height extracted by the UAV, corrected; is the height extracted by the UAV, and is the ratio obtained for the size class *j*.

Survival

The estimation of survival of the UAV and QFI plots was performed using the ratio model, demonstrated by Péllico Netto and Behling, (2019), expressed in Equation 3.

$$\hat{R} = \frac{\sum_{i=1}^{n} y_i}{\sum_{i=1}^{n} x_i} \quad (3)$$

Where: $\hat{R}$ is the estimated angular coefficient (ratio); x_i is the expected number of trees per hectare obtained in plot *i*; y_i is the real number of trees per hectare in plot *i*.

To verify the accuracy of the survival values generated by the UAV approach in relation to the QFI, the calculation of the confidence interval (CI) was performed. The confidence interval presents the amplitude of the average for the data, generated from the lower and upper limits (Péllico Netto and Brená 1997). For this, the survival per hectare was calculated (Equation 4) along with the CI for the UAV approach and for the QFI (Equation 5):

$$\hat{\bar{Y}} = \frac{\sum_{i=1}^{n} \hat{R}\, x_i}{n} \quad (4)$$

$$I = \hat{\bar{Y}} \pm t\sqrt{s_{\bar{Y}}^2} \quad (5)$$

Where: $\hat{R}$ is the estimated angular coefficient (ratio); x_i is the expected number of trees per hectare obtained in plot *i*; $\bar{Y}$ is the average of the estimate of trees per hectare; *n* is the number of plots. It is the trust interval; $\bar{Y}$ is the average of the trees estimate per hectare; *t* is the value of t-Student statistics at a significance level (α) of 0.01 and n^{-1} degrees of freedom, and $s_{\bar{Y}}^2$ is the estimated variance of the number of trees per hectare.

To determine whether the survival estimates obtained by the UAV approach were satisfactory, the following assumptions were applied:

H_0: $\hat{\bar{Y}}_e = \hat{\bar{Y}}_o$, indicates that the estimates generated by the UAV approach do not differ statistically from the QFI estimates. In this case, the average number of trees per hectare estimated by UAV should be within the confidence interval of the QFI.

H_1: $\hat{\bar{Y}}_e \neq \hat{\bar{Y}}_o$, indicates that the estimates generated by the UAV approach differ statistically from the QFI estimates. In this case, the average number of trees per hectare estimated by UAV is outside the confidence interval of the QFI.

Kernel Failure Surface

After H_0 was accepted (H_0: $\hat{\bar{Y}}_e = \hat{\bar{Y}}_o$), the Kernel Failure Surface (FSK) was generated for each plantation. This failure surface (Layer) had as reference the failures identified in the total area of the plantations (Census).

For this, the Kernel method was done using the Kernel Density tool in a GIS environment. The input parameters employed were cell size 0.5, search radius of 75 for plantations A and B and 100 for plantation C, and the area unit hectares to obtain the concentration of faults per hectare.

Then, using a raster calculator tool, the fault values were converted to a scale from 0 to 1 (standardisation), and the closer to 1, the lower the number of faults in the area, according to Equation 6.

$$x_{ip} = \frac{x_{max} - x_i}{x_{max}} \quad (6)$$

Where: x_{ip} is the estimated value of standardised failures (0 to 1) at the pixel; x_{max} is the estimated maximum value of failures obtained at the Kernel surface, in hectares; and x_i is the estimated value of pixel failure at the Kernel surface, given in hectares.

Uniformity measures

To obtain the uniformity indices (UI) of the plantations, the following indices were calculated in the R software environment: Coefficient of Variation in percentage ($VC_{\%}$); Gini coefficient (G) and accrued percentage of the densitometric variable of interest (50%) of the smaller trees planted (PV50) and their variations such as PV25 and PV75, with 25% and 75% of the smallest planted trees, respectively.

The PV variations were calculated using 25%, 50%, and 75% of the data, according to Equations 7, 8, and 9, respectively, taking into account the plantation failures. When calculated with the height (H) values, this index was called PH and when calculated with the canopy area values (Ca), it was called PCa.

$$PV25_j = \frac{\sum_{i=1}^{\frac{n_j}{4}} x_i}{\sum_{i=1}^{n_j} x_i} \quad (7)$$

$$PV50_j = \frac{\sum_{i=1}^{\frac{n_j}{2}} x_i}{\sum_{i=1}^{n_j} x_i} \quad (8)$$

$$PV75_j = \frac{\sum_{i=1}^{\frac{3n_j}{4}} x_i}{\sum_{i=1}^{n_j} x_i} \quad (9)$$

Where: $PV25_j$ is the accrued percentage of the densitometric variable of interest (H or Ac) of the 25% smallest trees planted from plot *j*; $PV50_j$ is the accrued percentage of the densitometric variable of interest (H or Ac) of the 50% smallest trees planted from plot *j*; $PV75_j$ is the accrued densitometric variable of interest (H or Ac) of the 75% smallest trees planted from plot *j*; x_i is the value of the densitometric variable of interest; n_j = number of planted trees arranged in ascending order (from the smallest one to the biggest one) at plot *j*.

For calculating the coefficient of variation percentage ($VC_{\%}$) and the Gini coefficient (G) all the data bank measures were employed, except the plantation failures. For calculating G (Equation 10) the ineq statistic package Zeileis et al. (2009) from the R software was employed R Core Team, (2022), and Equation 11 was employed for obtaining the $VC_{\%}$:

$$G_j = 1 - \sum_{i=0}^{n-1}(A_{j_{i+1}} - A_{j_i})(D_{j_{i+1}} - D_{j_i}) \quad (10)$$

$$VC_{\%j} = \frac{s_j}{\bar{x}_j}100 \quad (11)$$

Where: G_j is the Gini coefficient of the densitometric variable of interest in plot *j*; A_j = accrued rate of the number of trees from plot *j*; D_{ij} = accrued rate of the value of the densitometric variable of interest from plot *j*; $VC_{\%j}$ is the variation coefficient of the densitometric variable of interest at plot *j*; s_j is the standard deviation of the densitometric variable of interest at plot *j*; $\bar{x}_j$ is the average of the densitometric variable of interest in plot *j*.

For further assessment of the indices, knowing the variation range of each index, standardisation of its values was performed using the expressions described in Table 3, so that the resulting values were on the same 0 to 1 scale, considering that the closer the value to 1, the higher the uniformity.

Where: IU is the uniformity index; upper limit corresponds to the maximum uniformity of the index; lower limit is the value corresponding to the inexistence of uniformity; x_{ip} standardised index value (0 to 1) at the plot; x_{max} is the maximum value of the index obtained in the plantation's plots, and x_i is the value of the index obtained in the plot.

TABLE 3: Information on UAV flights over *Eucalyptus* sp. plantations.

IU	Lower limit	Upper limit	Standardisation
PV25	0	0.25	$x_{ip} = 4x_i$
PV50	0	0.50	$x_{ip} = 2x_i$
PV75	0	0.75	$x_{ip} = 4/3 * x_i$
G	1	0	$x_{ip} = 1 - x_i$
$VC_{\%}$	∞	0	$x_{ip} = (x_{max} - x_i)/x_{max}$

Uniformity surfaces

The uniformity indices of the rectangular plots of QFI and UAV (Sampling V1) were calculated, based on the variable height (*H*) (QFI) and the variables corrected height (H_{corr}) and canopy area (*Ca*) (UAV). The uniformity indices were divided into 3 plot frequency classes, and the number of classes was arbitrarily defined. To compare the frequency of plots per class resulting from the UAV approach with the QFI, the chi-square (χ^2) test was employed (Equation 12).

$$X^2 = \frac{\Sigma(F_o - F_e)^2}{F_e} \quad (12)$$

The chi-square (χ^2) tests the following hypotheses:

(1) H_0: $F_e = F_o$, the UAV plot frequency is not different from the QFI plot frequency when p-value ≥α. Thus, the methods do not differ statistically at the 5% significance level (α =0.05), and

(2) H_1: $F_e \neq F_o$, the UAV plot frequency is different from the QFI plot frequency when p-value <α. Thus, the methods are statistically different at the 5% significance level (α = 0.05).

Then, the remaining heights were corrected for sampling - V2 plots. The uniformity indices PH25, PH50, PH75, $VC_{\%}$ and G were calculated and standardised. The standardised uniformity indices were imported into GIS software, where, by means of the Inverse Distance Weighting (IDW) tool, the uniformity surface of each index for each plantation was generated.

Using the raster calculator tool, a map algebra was performed, in which the layers of each index were integrated to generate a single Uniformity Surface (US, Equation 13) for each plantation. The Uniformity Surface with failures (USf, Equation 14), which considers the distribution of the failures in the plantation, was determined by adding the standardised Kernel Failure Surface (FSK) to the uniformity surface (US).

$$US = \frac{\sum_{i=1}^{n} UI_i}{n} \quad (13)$$

$$US_f = \frac{(\sum_{i=1}^{n} UI_i) + FS_K}{n} \quad (14)$$

Where: *US* is the uniformity surface from the integration of indices PH25, PH50, PH75, $VC_{\%}$, and G; *UI* is the uniformity index; US_f is the uniformity surface from the integration of indices PH25, PH50, PH75, $VC_{\%}$, and G and the FSK; UI_i is the layer of uniformity index *i*; FSK is the layer corresponding to the Kernel standardised failure surface; and *n* is the number of layers.

To determine the degree of uniformity of the plantings the two uniformity surfaces generated (US and USf) were classified into three uniformity classes: low, medium, and high (Table 4).

TABLE 4: Uniformity classes employed to classify the uniformity surfaces of the plantings.

Class	C1 – L	C2 – M	C3 – H
Description	Low	Medium	High
Range	<0.65	0.65 – 0.75	>0.75

Results

Survival

Survival estimates by inventory and UAV are shown in Table 5, where: $\hat{\hat{Y}}$ is the average of trees estimated per hectare; $\hat{R}$ is the estimated angular coefficient/ratio; $S^2_{\hat{Y}}$ = variance of the estimated number of trees per hectare; $S_{\hat{Y}}$ = standard error of trees estimate per hectare; $S_{yx\%}$ is the standard error of the estimate in percentage; I is the trust interval (trees/ha); $F_{\%}$ is the failure percentage; and $S_{\%}$ is the survival percentage. These survival estimates were obtained by the ratio model Péllico Netto and Behling, (2019) and suggest that:

> In Plantation A, with the UAV survey, the survival estimate was 92.9% and with the QFI, the survival was 100%, therefore, hypothesis ($\hat{\hat{Y}}_e = \hat{\hat{Y}}_o$) was rejected, showing that statistically for this plantation, there was a difference between the methods.
>
> Plantation B presented a higher survival percentage, both from estimates by the UAV and in the field inventory estimates, 96.5% and 98.5%, respectively. The UAV estimation of the average of live trees per hectare was 1,626, within the confidence interval (I) of the QFI, which was 1,659 ± 44. Thus, hypothesis H_0 was not rejected, showing that, for this plantation, the estimations by both methods did not statistically differ.
>
> Plantation C presented 94.6% and 93.8% survival, for estimates of QFI and UAV, respectively. The average of live trees per hectare estimated by the UAV was 1,580 and it was within the trust interval of the field inventory (1,593 ± 121). Thus, hypothesis H_0 was not rejected, since the estimates did not statistically differ.

Uniformity

The χ^2 test revealed that there was no difference between the indices PV25, PV50 and G, calculated with the height (QFI) and the variable canopy area (UAV). Thus, for these cases, the hypothesis H_0: $F_e = F_o$ was not rejected, showing there was no significant difference between these indices (Table 6). When we compared the uniformity indices calculated with H (QFI) and H_{corr} (UAV), there was no significant difference between the methods in all indices (PV25, PV50, PV75, $VC_{\%}$ and G), where: NS is not significant; S is significant. PH25, PH50, and PH75 are the accrued height percentages in 25%, 50%, and 75% of the smaller trees planted; PCa25, PCa50, and PCa75 are the accrued percentage of the canopy area in 25%, 50% and 75%, of the smaller trees planted; $VC_{\%}$ is the coefficient of variation in percentage, and G is the Gini coefficient.

The application of height correction in Sampling V2 resulted in an increase in the standard deviation of the corrected variable in all plantations. However, the mean value and maximum and minimum values of the corrected heights were similar to those obtained from the field inventory (QFI) (Table 7), where: H is the height (m); H_{corr} is corrected height; Deviation is the standard deviation of the variable.

Thus, the corrected heights were employed to calculate the uniformity indices that showed no difference by the χ^2 test: PH25, PH50, PH75, $VC_{\%}$, and G (Table 8), where: Min is the minimum value of the index; A is the average value of the index; Max. is the maximum value of the index; D is the standard deviation of the index. PH25, PH50, and PH75 are the accrued height percentages in 25%, 50%, and 75% of the smaller trees planted; $VC_{\%}$ is the coefficient of variation in percentage, and G is the Gini coefficient.

Figure 3 presents the uniformity surfaces US and USf obtained for the three forest plantations targeted in this study, where the US were obtained based on Equation 13 and the USf were obtained based on Equation 14. The US and USf were classified into three uniformity classes: Low when the values were lower than 0.65 (red), Medium for values within the range of 0.65-0.75 (yellow), and High when the values were higher than 0.75 (green).

Figures 3-a, 3-c, and 3-e correspond to the US without planting failures for plantations A, B, and C, respectively. Figures 3-b, 3-d, and 3-f correspond to the USf, obtained for plantations A, B, and C, respectively. Thus, the US and

TABLE 5: Survival estimates by inventory and UAV.

Parameter	QFI			UAV		
	Plantation A	Plantation B	Plantation C	Plantation A	Plantation B	Plantation C
$\hat{\hat{Y}}$	1,670	1,659	1,593	1,551	1,626	1,580
$\hat{R}$	1.00	0.98	0.95	0.93	0.97	0.94
$S_{\hat{Y}}^2$	0	216	1,471	128	23	177
$S_{\hat{Y}}$	0	15	38	11	5	13
$S_{yx\%}$	0.0%	2.7%	7.6%	7.2%	0.9%	2.7%
I	1,670	1,659 ± 44	1,593 ± 121	1,551 ± 112	1,626 ± 14	1,580 ± 42
$F_{\%}$	0	1.5	5.4	7.1	3.5	6.2
$S_{\%}$	100	98.5	94.6	92.9	96.5	93.8

TABLE 6: Result of χ^2 test using the plot frequencies in the uniformity classes of the plantation uniformity indices.

Index QFI × UAV	p-value	Test	Index QFI × UAV	p-value	Test
PH25 × PH25	0.3055	NS 5%	PH25 × PCa25	0.2203	NS 5%
PH50 × PH50	0.7236	NS 5%	PH50 × PCa50	0.6437	NS 5%
PH75 × PH75	0.1023	NS 5%	PH75 × PCa75	0.0294	S 5%
$VC_{\%} \times VC_{\%}$	0.1202	NS 5%	$VC_{\%} \times VC_{\%}$	0.0110	S 5%
G × G	0.5524	NS 5%	G × G	0.4005	NS 5%

TABLE 7: Descriptive statistics of the height variable extracted from UAV images, before and after correction.

Statistics	*H* (m) QFI			*H* (m) UAV			H_{corr} (m) UAV		
	A	B	C	A	B	C	A	B	C
Minimum	0.00	0.00	0.00	0.00	0.00	0.00	0.00	0.00	0.00
Average	6.10	5.68	5.01	3.04	1.94	1.59	5.38	6.05	4.66
Maximum	8.10	7.10	7.00	7.12	7.60	3.89	9.46	16.63	8.84
Deviation	2.14	0.94	1.38	2.04	1.69	0.95	2.66	3.56	1.98

TABLE 8*:* Descriptive statistics of the uniformity indices before and after the standardisation.

Plantation	Index	Min	A.	Max.	D	Min.	A.	Max.	D
A	PH25	0.00	0.20	0.23	0.07	0.00	0.56	0.93	0.30
A	PH50	0.19	0.38	0.48	0.09	0.38	0.76	0.95	0.17
A	PH75	0.49	0.65	0.73	0.07	0.65	0.87	0.98	0.09
A	$VC_{\%}$	3.65	18.89	59.45	16.42	0.39	0.80	0.96	0.17
A	G	0.03	0.16	0.43	0.12	0.57	0.84	0.97	0.12
B	PH25	0.00	0.10	0.22	0.07	0.00	0.39	0.88	0.28
B	PH50	0.04	0.30	0.46	0.01	0.08	0.60	0.91	0.20
B	PH75	0.34	0.56	0.70	0.09	0.45	0.75	0.94	0.12
B	$VC_{\%}$	5.62	45.06	77.36	18.11	0.20	0.53	0.94	0.19
B	G	0.03	0.28	0.57	0.13	0.43	0.72	0.97	0.13
C	PH25	0.00	0.12	0.21	0.07	0.00	0.48	0.85	0.29
C	PH50	0.06	0.35	0.44	0.10	0.12	0.70	0.89	0.20
C	PH75	0.26	0.63	0.71	0.09	0.35	0.84	0.94	0.12
C	$VC_{\%}$	8.53	23.02	96.73	18.46	0.00	0.76	0.91	0.19
C	G	0.05	0.20	0.61	0.13	0.39	0.80	0.95	0.13

USf show differences in their presentation, as the former does not consider planting failures in its calculation, while the latter does.

For each of the plantations, the descriptive statistics of the uniformity surface (US and USf) are presented in Table 9, where: US is the surface with the bands' involving the average of all calculated indices; USf is the bands' calculation involving the uniformity indices average and the standardised Kernel failures surface; Min is the minimum value at the surface; A is the average value at the surface; Max. is the maximum value at the surface; D is the standard deviation of the values at the surface.

The area occupied by each uniformity class is presented in Table 10, where: US is the surface with the bands' calculation involving the average of all calculated indices; USf is the bands' math involving the uniformity indices average and the standardised Kernel failures.

According to the US, plantation A showed the highest percentage of the uniform productive area, 59.94%, followed by plantations C and B, with 37.34% and 0.52%, respectively. Plantation A was classified as a high uniformity plantation (C3), plantation C, medium uniformity (C2) and plantation B, low uniformity (C1).

When considering USf, plantation A remained with the highest percentage of uniform productive area (33.55%), followed by plantations C and B, with 24.35% and 0.49%, respectively. Plantation A was now classified as a medium uniformity plantation (C2), and plantations C and B remained with the same classification, C2 and C1, respectively.

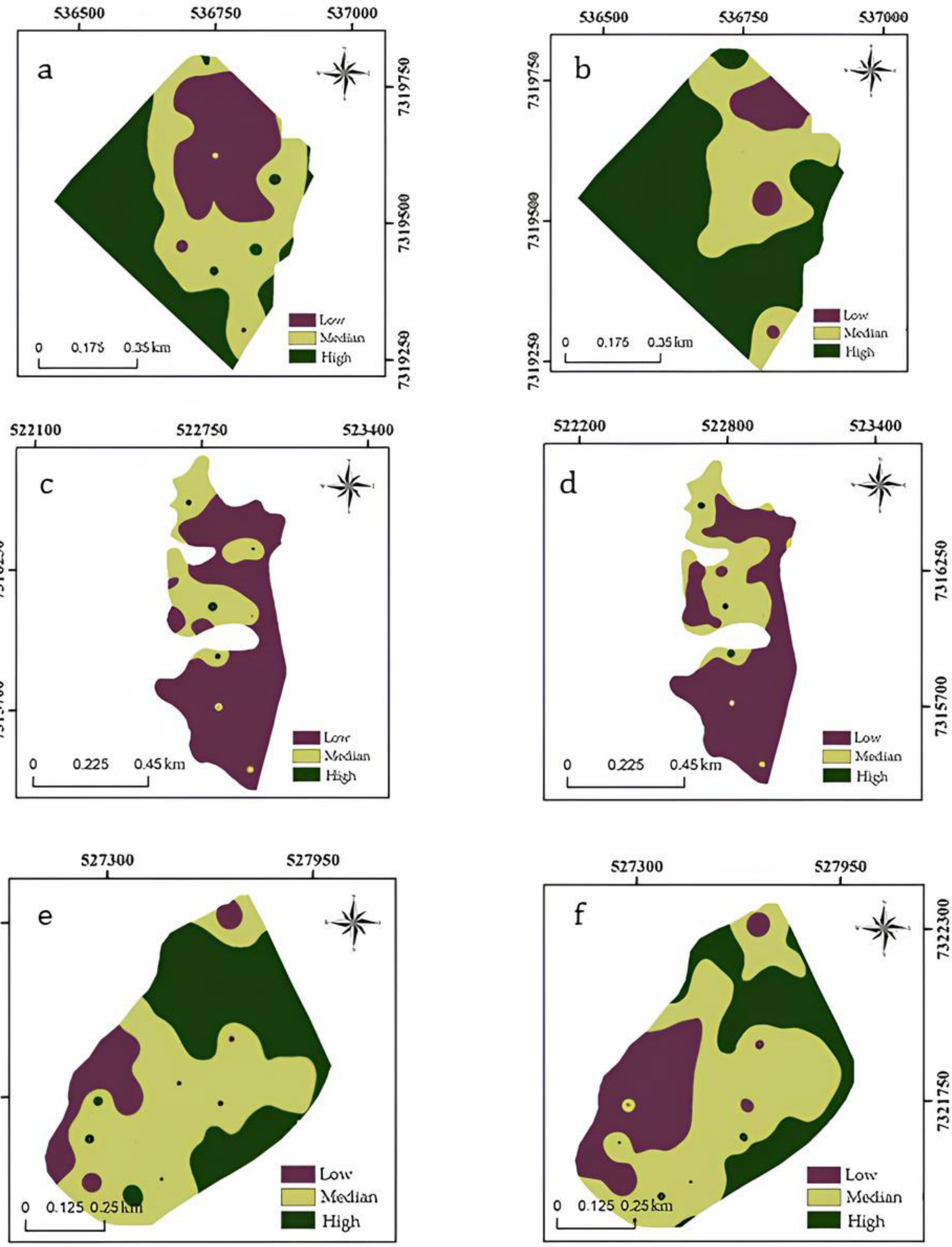

FIGURE 3: Uniformity surfaces obtained for plantation A: (a) US and (b) USf for plantation B: (c) US and (b) USf and plantation C: (e) US and (f) USf.

TABLE 9: Descriptive statistics of the uniformity surfaces.

Statistics	US				USf			
	Min.	A	Max.	D	Min.	A	Max.	D
A	0.41	0.77	0.95	0.078	0.42	0.71	0.89	0.08
B	0.24	0.6	0.92	0.068	0.29	0.61	0.89	0.07
C	0.17	0.72	0.90	0.062	0.25	0.70	0.85	0.07

Discussion

Remotely piloted aircraft systems (UAV) have emerged as innovative tools for the remote and efficient acquisition of dendrometric data (Silva et al. 2015). Among the main advantages of using UAV are the diversity of methods, platforms, and sensors available for data collection, allowing for greater flexibility and adaptability to the specific conditions of each study. These technologies also enable the collection of information in hard-to-reach areas, where conventional approaches could become unfeasible or costly. Furthermore, the significant reduction in the costs of acquiring high-definition images, combined with the ability to obtain data with high spatial and temporal resolution, represents a considerable advancement compared to traditional forest inventory methods (Lima Neto et al. 2012; Banu et al. 2016; Almeida et al. 2021). However, it is essential to emphasise that flight parameters and the quality of the generated cartographic products can influence the accuracy of the extracted attributes, especially regarding tree height.

In this study, the cartographic products obtained from UAV were initially used to assess the survival of the analyzed plantations and to obtain variables such as crown area and tree height. The results showed that, for plantations B and C, the survival estimates obtained from UAV were within the confidence interval calculated for the QFI. Plantation B had a survival rate of 96.5% according to UAV compared to 98.5% according to QFI, while plantation C showed 93.8% survival from UAV and 94.6% from QFI (Table 5). This consistency in results indicates that the estimates from both methods did not differ statistically. Additionally, the range of survival estimates calculated from UAVs was lower than that of the QFI for these two plantations.

In a study conducted by Zhao et al. (2021), a new algorithm was proposed for detecting planting failures and calculating the survival of young *Eucalyptus* sp. plantations based on images obtained from a passive sensor mounted on a UAV. The authors achieved acceptable results, with a failure detection rate exceeding 90% using the proposed methodology. Furthermore, they pointed out that identifying failures in an orthophoto is an excellent tool for monitoring survival rates in large forest plantation areas. Thus, UAVs are a promising alternative for survival estimates.

However, in plantation A, the QFI data indicated a survival rate of 100%, while the UAV recorded 92.9%. This discrepancy can be attributed to the fact that the survival calculation for the QFI was performed on three rectangular plots of relatively small area (~120 m^2), while the UAV estimates were based on three circular plots of one hectare. Consequently, the low sampling intensity and the small area of the QFI plots compromised the representativeness of the field inventory, which did not adequately capture the spatial variability of the plantation or the survival percentage. For this reason, plantation A was not used to assess whether UAV are an appropriate approach for survival estimates.

Regarding the crown area variable, the results indicated that the variable obtained from the UAV was not suitable for calculating uniformity indices, as significant statistical differences were observed between the UAV and QFI methods for the PCa75 and $VC_{\%}$ indices (Table 6). However, we emphasise that this result only encompasses the context of the plantations evaluated in the present study. Therefore, we encourage further studies using this variable to cover other scenarios related to forest planting conditions.

In relation to the tree height variable obtained from the UAV, comparisons with the heights derived from the QFI revealed a systematic error with a tendency to underestimate the measurements. This situation is thought to occur because, in dense vegetation, the passive sensors mounted on the UAV had difficulty capturing the reflectance of the ground. Consequently, while the Digital

TABLE 10: Uniformity classes and their respective areas.

Plantation	MB	C1 – L		C2 – M		C3 – H		Total (ha)
		(ha)	(%)	(ha)	(%)	(ha)	(%)	
A	US	1.15	7.82	4.76	32.24	8.84	59.94	14.75
A	USf	4.07	27.61	5.73	38.84	4.95	33.55	14.75
B	US	28.08	73.14	10.11	26.34	0.20	0.52	38.39
B	USf	25.87	67.39	12.33	32.12	0.19	0.49	38.39
C	US	6.21	11.45	27.75	51.21	20.23	37.34	54.19
C	USf	12.76	23.55	28.23	52.10	13.19	24.35	54.19

Surface Model (DSM) could be obtained clearly, this may not have been the case with the Digital Elevation Model (DEM), which could compromise the generation of the Canopy Height Model (CHM) and, consequently, the heights extracted from this cartographic product. To overcome this limitation, it is suggested that an existing DEM of the area, obtained before the planting was implemented, be used. Another alternative proposed in this study is the application of a size class correction factor (R_j, Equation 1) on the heights obtained from the UAV, based on field measurements. The application of this factor was evaluated by calculating the uniformity indices with the corrected heights (H_{corr}, Equation 2), allowing for a comparison between the uniformity indices obtained from the UAV and those generated by the QFI.

The results obtained from the UAV-corrected heights in calculating the uniformity indices in young *Eucalyptus* sp. plantations were promising, confirming that the uniformity indices PH25, PH50, PH75, $CV_{\%}$, and G did not present statistically significant differences compared to the values generated by the QFI (Table 6). Thus, the UAV-corrected heights are compatible with the heights collected in the field, and the proposed workflow for calculating the uniformity indices demonstrated statistically reliable results. Previous studies, such as those by Hentz et al. (2018) and Almeida et al. (2021), corroborate these findings by calculating different uniformity indices in forest plantations using UAV-derived heights. The authors conclude that the UAV photogrammetry technique is a promising tool for forest inventory, providing an effective alternative to traditional methods.

Thus, the use of UAV enabled the calculation of uniformity indices with a higher sampling intensity, increasing the number of plots employed in the calculations. This, in turn, resulted in a more representative coverage of the planted areas, allowing for uniformity index values that better reflect the reality of the plantations. McGown et al. (2016) suggested that the assessment of planting structure should be performed using multiple uniformity measures or the combination of different indices for a more robust analysis. In this study, the uniformity indices calculated with the greater sampling intensity were standardised (Table 8), allowing for their spatial integration and the generation of uniformity surfaces, both considering planting failures (USf) and without them (US) (Figure 3).

The analysis of US revealed significant patterns regarding the heterogeneity of tree heights in the three evaluated plantations. The greatest variability was identified in plantation B, classified as having low uniformity, indicating that various factors, such as competition for limited resources, soil conditions, and seedling quality, can impact plant growth. For instance, seedlings with inadequate genetic traits or poorly adapted to local conditions may lead to irregular development, contributing to the observed heterogeneity. In contrast, plantations C and A showed medium and high levels of uniformity, respectively, suggesting that tree heights in these locations are more homogeneous, indicating a more efficient forest management adapted to environmental conditions.

The inclusion of failure surface analysis in the uniformity evaluation demonstrated a significant shift in uniformity patterns across the plantations. Plantation A, which initially exhibited high uniformity (US), had its classification altered to medium when considering planting failures (USf). This change emphasises the importance of accounting for failures when assessing uniformity, as areas with absent trees or irregular growth affect the spatial distribution of the remaining trees. Thus, the USf analysis provides a more realistic view of plantation conditions, allowing for a deeper understanding of growth dynamics and the factors contributing to variability. This integrated approach is essential for developing management strategies that minimise failures and maximise uniformity, ultimately enhancing the productivity of plantations.

The literature indicates that low uniformity may be linked to various factors, including heterogeneity of environmental conditions, competition between trees, and quality of planted seedlings (Resende et al. 2018). Planting density and site quality are also significant influences (Sun et al. 2018). Failures along planting rows, for example, encourage asymmetric growth of adjacent trees and result in irregular competition, which is detrimental to the uniform development of vegetation (Ackerman et al. 2013). This situation increases the heterogeneity in tree heights and, consequently, decreases the overall uniformity of the plantation.

The high concentration of failures in certain areas can negatively impact uniformity, as locations classified as having low uniformity also tend to exhibit lower tree survival. This occurs because a plantation with numerous failures does not provide homogeneous conditions for tree establishment, leading to uneven competition for resources such as light, water, and nutrients (Ackerman et al. 2013). Therefore, forest management should focus efforts on medium and low uniformity classes, prioritising interventions that reduce failures and promote more uniform growth.

Stape et al. (2010) observed a positive correlation between initial uniformity at two years and final productivity at six years in clonal *Eucalyptus* sp. plantations. This relationship suggests that uniformity in the early development stages is a crucial indicator of future productive potential, where unequal resource availability, especially in the initial growth phase, can intensify competition between individuals, resulting in a heterogeneous plantation. Such irregular competition can undermine the uniform development of trees and the efficiency of resource use. Thus, it is recommended that survival studies be conducted alongside uniformity assessments, as this information may be critical for implementing forest management recommendations. By integrating these analyses, forest managers can make more informed decisions that enhance uniformity and, consequently, improve the productivity and quality of plantations.

In a study of a young *Eucalyptus* sp. plantation located in Espírito Santo, Brazil, Luu et al. (2013) found that reductions in the potential growth of trees varied from 2% in highly uniform locations to nearly 10% in areas of low uniformity, resulting in an overall decrease of 4.3% in the potential growth of the stand. The authors argue that silvicultural systems designed to maximise tree size uniformity could lead to a 5% to 15% increase in production at the stand level. Furthermore, this uniformity contributes to a more consistent supply of resources and improves tree quality. Conversely, Stape et al. (2010) indicate that tree size heterogeneity can reduce stand-level production by 10% to 18%. This finding reinforces the importance of maintaining a uniform structure in plantations, not only for immediate productivity but also for the long-term sustainability of forestry operations.

However, the lack of detailed silvicultural reports in our study hampered a deeper analysis of the possible causes of spatial variability in uniformity within the plantations. The absence of data on management practices, such as fertilisation, irrigation, and pest control, limited our understanding of how these factors influenced vegetation structure. For a more comprehensive understanding of uniformity in plantations, it is suggested that this variable be assessed alongside silvicultural reports that include data on replanting, fertilisation, pest control, and competition with weeds. By combining uniformity surfaces with field data, a more accurate view of the influences affecting stand uniformity can be obtained. Integrating these data will allow for the identification of management practices that can be adjusted to maximise plantation quality and productivity.

Conclusions

The research conducted demonstrated the effectiveness of using UAV in obtaining dendrometric data and assessing uniformity in *Eucalyptus* sp. plantations. The results showed that the survival estimates obtained from the UAV were statistically comparable to those obtained through QFI in plantations B and C, highlighting the viability of this technology for forest monitoring. Additionally, the analysis of uniformity surfaces revealed significant patterns in the heterogeneity of tree heights, suggesting that initial uniformity is a critical factor for future productivity.

However, the findings also emphasised the need for an integrated approach when considering planting failures in the uniformity assessment, as the presence of these failures can compromise the analysis of stand structure. For future studies, it is essential to consider the inclusion of silvicultural reports that encompass management practices such as fertilisation, pest control, and irrigation, to achieve a more comprehensive understanding of the dynamics influencing uniformity and tree growth. This integration of data will allow for the formulation of more robust recommendations for forest management.

The implications of this research are clear: the use of UAV can not only optimise forest inventory processes but also provide valuable information for the sustainable management of plantations. The adoption of this technology may lead to significant improvements in the productivity and quality of plantations, contributing to the development of more efficient forestry practices. The importance of maintaining adequate uniformity is not limited to immediate productivity but is also essential for the long-term sustainability of forestry operations. In summary, this study not only confirms the relevance of UAV in forest management but also establishes a solid foundation for future investigations that may further explore the potential of this technology in different contexts and planting conditions.

Competing interests

The authors declare that they have no competing interests.

Authors'contributions

AAM: conceptualisation, methodology, software, validation, formal analysis, investigation, resources, data curation, writing—original draft preparation and visualisation.

APDC: conceptualisation, methodology, software, validation, formal analysis, investigation, resources, data curation, writing—original draft preparation, visualisation, supervision, project administration and funding.

AB: conceptualisation, methodology, software, validation, formal analysis, investigation, resources, data curation, writing—original draft preparation and visualisation.

RM: conceptualisation, methodology, software, validation, formal analysis, investigation, resources, data curation, writing—original draft preparation and visualisation.

KE: conceptualisation, methodology, software, validation, formal analysis, investigation, resources, data curation, writing—original draft preparation and visualisation.

CN: conceptualisation, methodology, software, validation, formal analysis, investigation, resources, data curation, writing—original draft preparation and visualisation.

IDSB: conceptualisation, methodology, software, validation, formal analysis, investigation, resources, data curation, writing—original draft preparation and visualisation.

JASF: conceptualisation, methodology, software, validation, formal analysis, investigation, resources, data curation, writing—original draft preparation and visualisation.

JWT: conceptualisation, methodology, software, validation, formal analysis, investigation, resources, data curation, writing—original draft preparation and visualisation.

GAO: conceptualisation, methodology, software, validation, formal analysis, investigation, resources, data curation, writing—original draft preparation and visualisation.

Acknowledgements

The authors thank the company Klabin S.A. for providing the data

References

Ackerman, S.A., Ackerman, P.A., & Seifert, T. (2013). Effects of irregular stand structure on tree growth, crown extension and branchiness of plantation grown *Pinus patula. Southern Forests: a Journal of Forest Science*, *75*(4), 247-256. http://dx.doi.org/10.2989/20702620.2013.846722

Almeida, A., Gonçalves, F., Silva, G., Mendonça, A., Gonzaga, M., Silva, J., Souza, R., Leite, I., Neve, K., Boeno, M., & Souza, B. (2021). Individual tree detection and qualitative inventory of a *Eucalyptus* sp. stand using UAV photogrammetry data. *Remote Sensing*, *13*(18), 3655. http://dx.doi.org/10.3390/rs13183655.

Aspinwall, M.J., King, J.S., McKeand, S.E., & Bullock, B.P. (2011). Genetic effects on stand level uniformity and above-and belowground dry mass production in juvenile loblolly pine. *Forest Ecology and Management, 262*(4), 609-619. https://doi.org/10.1016/j.foreco.2011.04.029

AGEFLORE - Associação Gaúcha de Empresas Florestais. (2020). [O Setor de Base Florestal no Rio Grande do Sul]. http://www.ageflor.com.br/noticias/wp-content/uploads/2020/12/O-Setor-de-Base-Florestal-no-Rio-Grande-do-Sul-2020-ano-base-2019.pdf . Accessed: July 20, 2024.

Banu, T.P., Borlea, G.F., Banu, C. (2016). The use of drones in forestry. *Journal of Environmental Science and Engineering, 5*(11), 557-562. https://doi.org/10.17265/2162-5263/2016.11.007.

Binkley, D., Stape, J.L., Bauerle, W.L., & Ryan, M.G. (2010). Explaining growth of individual trees: light interception and efficiency of light use by *Eucalyptus* at four sites in Brazil. *Forest Ecology and Management, 259*(9), 1704-1713. https://doi.org/10.1016/j.foreco.2009.05.037

Binkley, D., Stape, J.L., Ryan, M.G., Barnard, H.R., & Fownes, J. (2002). Age related decline in forest ecosystem growth: an individual tree, stand structure hypothesis. *Ecosystems*, *5*, 58-67. https://doi.org/10.1007/s10021-001-0055-7

Climate-Date.Org. Dados climáticos para cidades mundiais. https://pt.climate-data.org/america-do-sul/brasil/parana/telemacoborba-765176/. 28 Oct. 2024.

Dalla Corte, A.P., Rex, F.E., Almeida, D.R.A.D., Sanquetta, C.R., Silva, C.A., Moura, M.M., Wilkinson, B., Zambrano, A.M.A., Neto, E.M.C., Veras, H.F.P., Moraes, A., Klauberg, C., Mohan, M., Cardil, A., & Broadbent, E.N. (2020). Measuring individual tree diameter and height using GatorEye High Density UAV-Lidar in an integrated crop-livestock-forest system. *Remote Sensing*, *12*(5), 863. https://doi.org/10.3390/rs12050863

Gonçalves, J.D.M., Alvares, C.A., Behling, M., Alves, J.M., Pizzi, G.T., & Angeli, A. (2014). Produtividade de plantações de eucalipto manejadas nos sistemas de alto fuste e talhadia, em função de fatores edafoclimáticos. *Scientia Forestalis*, *42*(103), 411-419. https://www.alice.cnptia.embrapa.br/alice/handle/doc/1005140

Hakamada, R. E., Stape, J.L., Lemos, C.C.Z.D., Emanuel, A., Almeida, A., & Silva, L.F. (2015a). Uso do inventário florestal e da uniformidade entre árvores como ferramenta de monitoramento da qualidade silvicultural em plantios clonais de eucalipto. *Scientia Forestalis*, *43*(105), 27-39. https://www.ipef.br/publicacoes/scientia/nr105/cap03.pdf

Hakamada, R.E., Stape, J.L., Lemos, C.C.Z.D., Almeida, A.E.A., & Silva, L.F. (2015b). Uniformidade entre árvores durante uma rotação e sua relação com a produtividade em *Eucalyptus* clonais. *Cerne*, *21*, 465-472. https://doi.org/10.1590/01047760201521031716

Hentz, Â.M., Silva, C.A., Dalla Corte, A.P., Netto, S.P., Strager, M.P., & Klauberg, C. (2018). Estimating forest uniformity in *Eucalyptus* spp. and *Pinus taeda* L. stands using field measurements and structure from motion point clouds generated from unmanned aerial vehicle (UAV) data collection. *Forest Systems*, *27*(2), e005-e005. https://doi.org/10.5424/fs/2018272-11713

IBÁ – Indústria Brasileira de Árvores. (2022) [Relatório Anual 2022]. Available from: https://iba.org/datafiles/publicacoes/relatorios/relatorio-anual-iba2022 compactado.pdf. Accessed: July 20, 2024.

IBÁ – Indústria Brasileira de Árvores. (2019) [Relatório 2019]. https://iba.org/datafiles/publicacoes/relatorios/iba-relatorioanual2019.pdf. Accessed: July 20, 2024.

Lima Neto, E.M., Biondi, D., Araki, H., & Bobrowski, R. (2012). Fotografias aéreas para mensuração da área de copa das árvores de ruas de Curitiba - PR. *Floresta*, *42*(3), 577-586. https://doi.org/10.5380/rf.v42i3.23944

Luu, T.C., Binkley, D., & Stape, J.L. (2013). Neighborhood uniformity increases growth of individual *Eucalyptus* trees. *Forest Ecology and Management*, *289*, 90-97. https://doi.org/10.1016/j.foreco.2012.09.033

McGown, K.I., O'Hara, K.L., & Youngblood, A. (2016). Patterns of size variation over time in ponderosa pine stands established at different initial densities. *Canadian Journal of Forest Research, 46*(1), 101-113. https://doi.org/10.1139/cjfr-2015-0096

Péllico Netto, S., & Behling, A. (2019). Additivity of tree biomass components using ratio estimate. *Anais da Academia Brasileira de Ciências*, *91*, e20180272. https://doi.org/10.1590/0001-3765201920180272

Péllico Netto, S, & Brena, D.A. (1997). Inventário Florestal. 316 p.

R Core Team. (2023). R: A Language and Environment for Statistical Computing. R Foundation for Statistical Computing version 4.2.3 (software). https://www.R-project.org/

Resende, R.T., Marcatti, G.E., Pinto, D.S., Takahashi, E.K., Cruz, C.D., & Resende, M.D.V. (2016). Intra-genotypic competition of *Eucalyptus* clones generated by environmental heterogeneity can optimize productivity in forest stands. *Forest Ecology and Management*, *380*, 50-58. https://doi.org/10.1016/j.foreco.2016.08.041

Resende, R.T., Soares, A.A., Forrester, D.I., Marcatti, G.E., dos Santos, A.R., Takahashi, E.K., Silva, F.F., Grattapaglia, D., Resende M.D.V. & Leite, H.G. (2018). Environmental uniformity, site quality and tree competition interact to determine stand productivity of clonal *Eucalyptus*. *Forest Ecology and Management*, *410*, 76-83. https://doi.org/10.1016/j.foreco.2017.12.038

Ryan, M.G., Stape, J.L., Binkley, D., Fonseca, S., Loos, R.A., Takahashi, E.N., Silva, C.R., Silva, S.R., Hakamba, R.E., Ferreira, J.M., Lima, A.M.N., Gava, J.L., Leite, F.P., Andrade, H.B., Alves, J.M. & Silva, G.G. (2010). Factors controlling *Eucalyptus* productivity: how water availability and stand structure alter production and carbon allocation. *Forest Ecology and Management*, *259*(9), 1695-1703. https://doi.org/10.1016/j.foreco.2010.01.013

Salamí, E., Barrado, C., & Pastor, E. (2014). UAV flight experiments applied to the remote sensing of vegetated areas. *Remote Sensing*, *6*(11), 11051-11081. https://doi.org/10.3390/rs61111051

Sanquetta, C.R., Corte, A.P.D., Pelissari, A.L., Tomé, M., Maas, G.C.B., & Sanquetta, M.N.I. (2018). Dinâmica em superfície, volume, biomassa e carbono nas florestas plantadas brasileiras: 1990-2016. *BIOFIX Scientific Journal*, *3*(1), 152-160. https://doi.org/10.5380/biofix.v3i1.58384

Silva, C.A., Souto, M.V.S., Duarte, C.R., Bicho, C.P., Sabadia, J.A.B. (2015). Avaliação da acurácia dos ortomosaico e modelos digitais do terreno gerados pelo MVANT/DNPM. *Revista Brasileira de Cartografia*, *67*(7), 1479-1495. http://www.repositorio.ufc.br/handle/riufc/64400. https://doi.org/10.14393/rbcv67n7-49200

Soares, A.A., Leite, H.G., Souza, A.L., Silva, S.R., Lourenço, H.M., & Forrester, D.I. (2016). Increasing stand structural heterogeneity reduces productivity in Brazilian *Eucalyptus* monoclonal stands. *Forest Ecology and Management*, *373*, 26-32. https://doi.org/10.1016/j.foreco.2016.04.035

Stape, J.L., Binkley, D., Ryan, M.G., Fonseca, S., Loos, R.A., Takahashi, E.N., Silva, C.R., Silva, S.R., Hakamanda, R.E., Ferreira, J.M.A., Lima, A.M.N., Gava, J.L., Leite, F.P., Andrade, H.B., Alves, J.M., Silva, G.G.C., & Azevedo, M.R. (2010). The Brazil *Eucalyptus* Potential Productivity Project: Influence of water, nutrients and stand uniformity on wood production. *Forest Ecology and Management*, *259*(9), 1684-1694. https://doi.org/10.1016/j.foreco.2010.01.012

Sun, H., Diao, S., Liu, R., Forrester, D., Soares, A., Saito, D., Dong, R. & Jiang, J. (2018). Relationship between size inequality and stand productivity is modified by self-thinning, age, site and planting density in *Sassafras tzumu* plantations in central China. *Forest Ecology and Management*, *422*, 199-206. https://doi.org/10.1016/j.foreco.2018.02.003.

Torresan, C., Berton, A., Carotenuto, F., Di Gennaro, S.F., Gioli, B., Matese, A., Miglietta, F., Vagnoli, C., Zaldei, A. & Wallace, L. (2017). *Forestry Applications of UAVs in Europe: A review. International Journal of Remote Sensing*, *38*(8-10), 2427-2447. https://doi.org/10.1080/01431161.2016.1252477

Yáñez, M.A., Fox, T.R., & Seiler, J.R. (2017). Silvicultural intensity and site effects on stand uniformity of loblolly pine varieties and families. *Forest Science*, *63*(6), 606-613. https://doi.org/10.5849/FS-2016-036R2

Zeileis, A., Kleiber, C., & Zeileis, M.A. (2009). Package 'ineq'. Technical Report. https://cran.r-project.org/web/packages/ineq/ineq.pdf

Zhang, C., & Kovacs, J.M. (2012). The application of small unmanned aerial systems for precision agriculture: a review. *Precision Agriculture*, *13*, 693-712. https://doi.org/10.1007/s11119-012-9274-5

Zhao, H., Wang, Y., Sun, Z., Xu, Q., & Liang, D. (2021). Failure detection in eucalyptus plantation based on UAV images. *Forests*, *12*(9), 1250. https://doi.org/10.3390/f12091250